Available online at www.sciencedirect.com
SCIENCE DIRECT®

Journal of the European Ceramic Society 24 (2004) 3419–3425
www.elsevier.com/locate/jeurceramsoc

Fabrication of complex-shaped alumina/nickel nanocomposites by gelcasting process

Koichi Niihara*, Bum-Sung Kim, Tadachika Nakayama, Takafumi Kusunose, Takuya Nomoto, Akio Hikasa, Tohru Sekino

The Institute of Scientific and Industrial Research, Osaka University, 8-1 Mihogahoka, Ibaraki, Osaka 567-0047, Japan

Abstract

Complex-shaped Al_2O_3/Ni nanocomposites with preserved multifunctional magnetic properties are successfully fabricated by a gelcasting process. Based on an investigation of the effects of suspension composition on the drying, debinding, and reduction-pressureless sintering processes, a stable Al_2O_3/NiO binary oxide aqueous suspension with optimal monomer, dispersant, and solid composition is defined. Wet gelcast bodies produced using this suspension system shrink by 4.72% during humidity-controlled drying, with a bending strength of the fully dried green body of 3.84 ± 0.84 MPa. The interconnected void structure of the debound green body provides hydrogen reduction of dispersed NiO without metamorphosis or shrinkage. Al_2O_3/Ni nanocomposites with complex shapes are successfully produced by pressureless sintering, and exhibit appropriate strength (586 ± 50 MPa) after 21.5% shrinkage. Dispersed Ni particles exhibit typical ferromagnetic behavior in the Al_2O_3 matrix. This study confirms that gelcasting is a viable process for fabricating industrially applicable Al_2O_3/Ni nanocomposites with balanced mechanical and magnetic properties.

Keywords: Al_2O_3; Gelcasting; Nanocomposites; Ni; Suspensions

1. Introduction

Much attention has been focused on the development of ceramic nanocomposites with nano-sized metal dispersion because such materials offer outstanding mechanical and multifunctional properties. The authors' group has already reported the synthesis of distinct and unusual ceramic/metal nanocomposite materials by hydrogen reduction and sintering from ceramic/metal oxide mixtures prepared by powder metallurgy or solution chemical routes.[1–4] As an example, Al_2O_3/metal nanocomposites fabricated by hydrogen reduction followed by hot pressing of Al_2O_3/metal oxide powder mixtures exhibit both high fracture strength and peculiar functional properties due to the dispersion of nano-sized metal particles.[5–9] However, these kinds of materials have previously been developed by reductive hot-pressing, and are difficult to machine as a consequence of the improved mechanical properties. The high machining costs for these materials therefore preclude widespread industrial application.

Near-net shaping has the potential to overcome these problems while maintaining the multi-functionality of the material. In near-net shaped materials, the suspension properties play a substantial role in determining the final properties of the specimen and the range of applications. Gelcasting is a novel process for the fabrication of complex-shaped ceramic green bodies from highly solid-loaded monomer-based aqueous suspensions. In this process, the monomer in the suspension is polymerized during casting. Well-dried and debound green bodies can then be densified by pressureless sintering. According to previous research, the use of a stable suspension and control of specific process conditions (drying, debinding, sintering) important aspects of this technique.[10–13] However, the mechanical properties of cast and pressureless-sintered products are often poorer than those produced by conventional sintering processes. Combination of an optimized nanocomposite material system and gelcasting process therefore represents a potentially useful method for producing strong, multifunctional specimens in industrially applicable shapes.

In the present study, the optimum suspension conditions and process route for the fabrication of complex-shaped Al_2O_3/Ni nanocomposites are investigated. Ni

* Corresponding author. Tel.: +81-6-6879-8441; fax: +81-6-6879-8444.
E-mail address: niihara@sanken.osaka-u.ac.jp (K. Niihara).

0955-2219/$ - see front matter © 2003 Elsevier Ltd. All rights reserved.
doi:10.1016/j.jeurceramsoc.2003.10.027

was selected as the dispersant in this study because of the potential magnetic functionality such a dispersion would offer as a ferromagnetic metal.[7,8]

The potential application of nanocomposites as novel structural or functional engineering materials depends heavily on the consolidation of powders into bulk materials. Numerous authors have shown that pressure-assisted sintering, such as hot-press sintering, is adequate for both reaching full density and preventing grain growth.[14] Pressureless sintering was necessarily used in the present investigation because of the lack of suitable pressure-assisted pressing processes for complex shapes, which are the target of this study. The relationship between the final specimen properties and the preparation conditions is investigated through systematic fabrication of gelcast Al_2O_3/Ni nanocomposite under various conditions of suspension synthesis, drying,[15,16] debinding, and reduction-sintering.[17,18]

2. Experimental procedures

2.1. Preparation of suspension

The solution chemical route was selected to obtain the Al_2O_3/NiO mixture powder.[4] High-purity $Ni(NO_3)_2{\cdot}6H_2O$ (nickel nitrate, 99.9%, Wako Pure Chem. Ind. Ltd., Japan) was used as the source material for Ni dispersion. Weighted nitrate powders, corresponding to 5 vol.% of nickel in the final composite, were initially dissolved in ethyl alcohol at 60 °C. Subsequently, α-Al_2O_3 (TM-DAR, 0.16 μm, 99.99% Taimei Chem. Co., Japan) powder was mixed with the nitrate solution and ball-milled for 24 h. The dried mixture was calcined at 400 °C in air to obtain a homogeneous Al_2O_3/NiO powder. The final Al_2O_3/nano-sized NiO mixture was wetted and dry ball-milled for 24 h.

In this aqueous gelcasting processing, methacrylamide (MAM, 98%, Sigma Chem. Co., USA) was used as the main monomer, and *N*,*N*'-methylenebisacrylamide (MBAM, 99%, Sigma Chem. Co., USA) was used as the cross-linker for making the organic solution. The premixed aqueous solution contained 1–8 wt.% total organic chemicals, and the mass ratio of MAM to MBAM was set at 5:1. To prepare 48.5–51.5 vol.% solid loading of suspensions, the weighted monomers were dissolved in deionized water for 24 h. For highly solid-loaded suspensions, poly-acrylic acid (SN Dispersant 5468, Sannopco Co. Japan) was added to the monomer solution as a dispersant for the Al_2O_3/NiO mixture, and dissolved over 1 h. The Al_2O_3/NiO mixture was then added to this solution and dispersed under stirring for 24 h.

The specific surface area of the Al_2O_3/NiO mixture was measured by the Brunauer-Emmett-Teller (BET) model[19] (Autosorb-1, Quantachrome Co.) through nitrogen adsorption. Rheological measurements were performed on a rotational stress-controlled rheometer (BM, Tokimec Inc. Tokyo, Japan) in the shear rate range of 1.74–17.4 s^{-1} at room temperature. The relationship between the rheological behavior, solid loading and quantities of monomer and dispersant were estimated, and the optimal suspension conditions were selected based on this relationship.

2.2. Characterizations of related processes

Drying was carried out in a relative humidity (RH) controlled chamber for de-molded specimens under conditions of 90% RH and 30 °C. For investigation of the drying behavior under these conditions, the weight loss and one-dimensional shrinkage of a rectangular specimen were measured. The debinding condition in air was determined by thermogravimetric and differential thermal analysis (TG-DTA) up to 500 °C. The fully dried and debound green body was reduced under hydrogen flow at 700 °C for 1 h, followed by continuous sintering at 1500 °C for 4 h under Ar.

The surface morphologies of the reduced green body and sintered specimen were observed by transmission electron microscopy (TEM; 200 kV, H-8100, Hitachi, Japan) and field-emission scanning electron microscopy (FE-SEM; S-5000, Hitachi, Japan). Magnetization curves of the nanocomposites were measured using a SQUID magnetometer at 27 °C.

3. Results and discussion

3.1. Characteristics of stable suspension

As a solution chemical route, a Al_2O_3/nano-sized NiO powder was successfully synthesized. BET measurement revealed a specific surface area of 12.08 m^2/g. In the gelcasting process, it is important maintain good flow properties of the highly solid-loaded suspension. It is not possible to synthesis a stable suspension simply by controlling pH alone, and the addition of a polymeric dispersant is necessary to stabilized the monomer solution. To determine the most appropriate amount of dispersant, leading to the best dispersion state, a 5 wt.% monomer suspension with solid loading of 50 vol.% Al_2O_3/NiO was prepared with different amounts of dispersant (Fig. 1). The results of these tests confirmed that the concentration of dispersant strongly influences the rheological behavior of the suspension. Below 1 wt.% dispersant, the viscosity exceeds the available measurement range (dotted line), but decreased rapidly with increasing dispersant content up to 1.75 wt.% at pH 7.5 in the Al_2O_3/NiO suspension. Further addition resulted in increased viscosity due to saturation of the particle surfaces with adsorbed PAA, which eliminates the

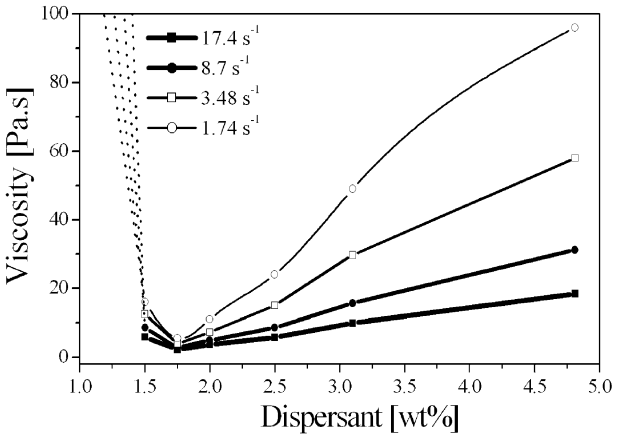

Fig. 1. Rheological behaviors of 5 wt.% monomer concentrated and 50 vol.% solid loaded suspension with different amount of dispersant (shear rate: 1.74–17.4 s^{-1}).

dependence of the suspension rheology on the PAA concentration. Negative electrostatic surface charge of both oxides was achieved at the present pH (~7.5), in accordance with the isoelectric points of α-Al_2O_3 and NiO of pH 8–9 and 10–11, respectively.[11] This electrostatic force, and the addition of PAA to increase steric repulsion, prevented phase segregation.

Fig. 2 shows the change in viscosity with solid loading of the Al_2O_3/NiO mixture for a monomer solution containing 1.75 wt.% PAA and 5 wt.% monomer. The viscosity increased slightly with solid loading up to 50 vol.%, and further addition to 51.5 vol.% resulted in a rapid increase in viscosity. The viscosity decreased with increasing shear rate from 1.74 to 17.4 s^{-1}. From the analysis at a given quantity of dispersant (Fig. 1) and solid concentration (Fig. 2), 1.75 wt.% PAA and 50 vol.% solid concentration were selected for further investigation of the Al_2O_3/NiO mixture suspension.

Fig. 3 shows the variation in viscosity (shear rate 3.48 s^{-1}) with total monomer content. The suspension contained 1.75 wt.% PAA and 50 vol.% Al_2O_3/NiO (solid loading). The viscosity decreased with increasing total monomer concentration up to 5 wt.%, and further addition resulted in an increase in viscosity. The monomer concentration range of 5–8 wt.% affords relatively low castable viscosities. From these results it is understood that the rheological behavior of inorganic suspensions also depend strongly on the monomer content. Following this investigation, monomer contents of 5 and 8 wt.% were chosen for subsequent processes.

The concentrations of monomer, dispersant, and solid are therefore confirmed to strongly influence the rheological behavior of the Al_2O_3/NiO suspension, and a suspension of 1.75 wt.% PAA, 50 vol.% solid, and 5–8 wt.% monomer can be selected as an optimized condition for the binary colloidal Al_2O_3/NiO mixture system.

3.2. Characteristics of specific processes

3.2.1. Humid drying

Prior to casting in the rectangular (64×43×12 mm) and complex-shaped molds, ammonium persulfate was tested as the initiator and *N,N,N′,N′*- tetramethylethylenediamine was examined as the catalyst. The wet body was dried in a humidity-controlled chamber because drying without humidity results in cracking due to non-uniform shrinkage. The drying weight-loss curves for specimens prepared with 5 and 8 wt.% monomer content are shown in Fig. 4 as plots of the fractional weight-loss (X) vs. time (t), where X is defined as the ratio of the instant weight loss, Δm, to the theoretical final weight loss, m_0, i.e. $X = \Delta m/m_0$. Both X vs. t plots exhibit a slight deviation from a linear relation at over $0.6X$, and weight losses can be seen to continue for up to 140 h. The weight loss rate of the 8 wt.% monomer suspension is higher than that of the 5 wt.% suspension.

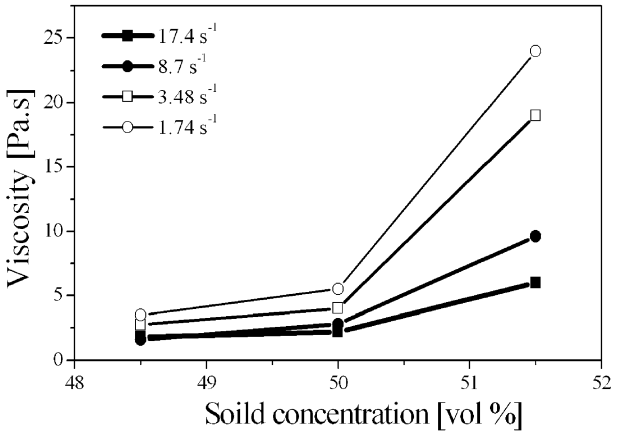

Fig. 2. Rheological behaviors of 5 wt.% monomer and 1.75 wt.% dispersant concentrated suspension with different solid loading (shear rate: 1.74–17.4 s^{-1}).

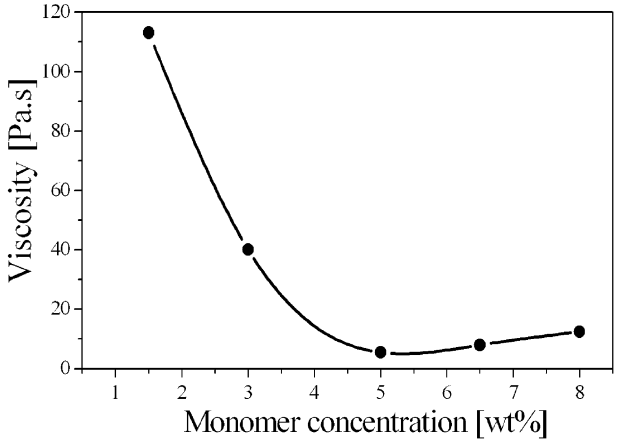

Fig. 3. Rheological behaviors of 1.75 wt.% dispersant concentrated and 50 vol.% solid loaded suspension with different amount of monomer (shear rate: 3.84 s^{-1}).

Fig. 5 shows the one-dimensional shrinkage curves for the wet bodies prepared with 5 and 8 wt.% monomer contents. Here, shrinkage is defined as the ratio of the measured length to the initial length (64 mm) of the rectangular specimen. Active shrinkage occurred in the initial 40 h. The maximum shrinkage reached 4.06 and 4.72% for the 5 and 8 wt.% monomer specimens, respectively. The bending strength of the green body was as high as 3.84 ± 0.84 MPa.

The physical mechanism of drying can be classified into three stages in gelcasting.[15] In the initial stage (constant rate period), the water is evaporated at a constant rate via capillary force to the surface of the green body. The green body thus shrinks at the rate of water evaporation. The gel matrix imparts a compressive stress, and particles become orientated. The initial linear drying range in the present study, the first 5 h, was confirmed as such a constant-rate drying period. The transition between the intermediate stage (falling rate period) and the final stage (polymer diffusion period) appears to occur at around 40 h, considering the relationships for weight loss (Fig. 4) and shrinkage (Fig. 5).

3.2.2. Debinding

The fully dried green bodies were debound to remove organic gel, as monitored by TG-DTA. Fig. 6 shows the debinding profile in air at 5 °C/min for the sample prepared with 5 wt.% monomer content. The fractional weight loss (α) of the dried body is defined as the ratio of the instant weigh loss, Δm, to the final weigh loss, m_f, i.e. $\alpha = \Delta m/m_f$. Residual water boiled near 100 °C, and organic gel was liberated between 250 and 500 °C. Thermal analysis revealed a debinding temperature of 400 °C. After debinding, the 8 wt.% monomer specimen had maintained a good shape, whereas the 5 wt.% monomer specimen exhibited fine micro-cracks in the center.

It is not clear in which process these micro-cracks originated, as the cracks may have been present but no visible after drying process, or may have been generated during the debinding process. However, it is believed that the monomer is not distributed homogeneously in the Al_2O_3/NiO green body at this lower concentration. This effect would result in an inhomogeneous stress distribution due to gas pressure (water vapor or organic compounds). Therefore, green bodies prepared with 8 wt.% monomer content were selected for final reduction and pressureless sintering.

3.2.3. Reduction and pressureless sintering

Gas-solid reaction of NiO reduction in the Al_2O_3/NiO debound body can proceed in this system because of the open internal structure. The reduction behavior in similar

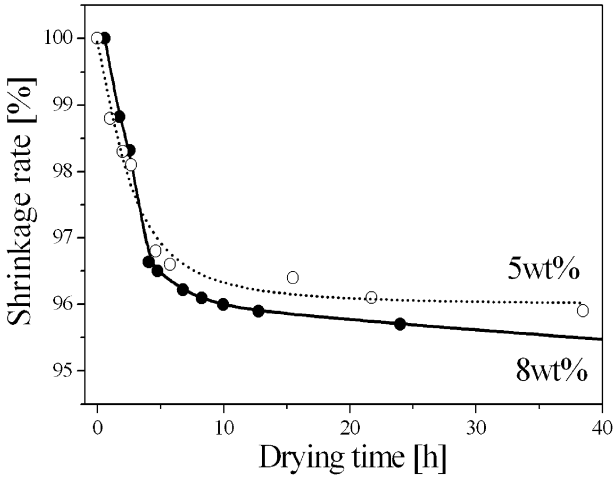

Fig. 5. The one-dimensional percent shrinkage behaviors of 5 and 8 wt.% monomer concentrated wet bodies (1.75 wt.% PAA, 50 vol.% solid loading) under the humidity control drying.

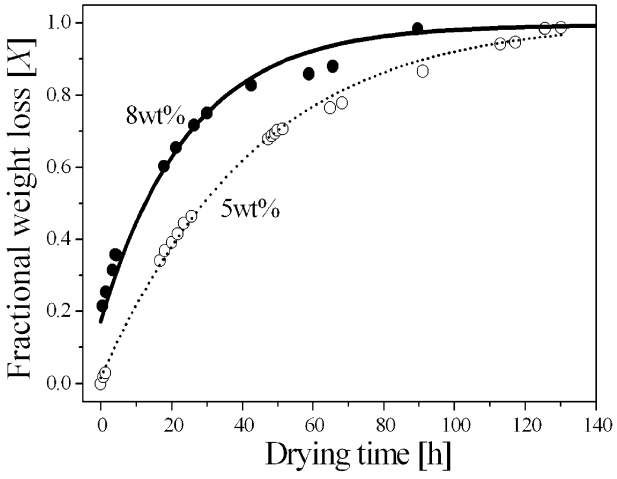

Fig. 4. The drying rates of 5 and 8 wt.% monomer concentrated wet bodies (1.75 wt.% PAA, 50 vol.% solid loading) as plots of the fractional weight loss (X) to time (t).

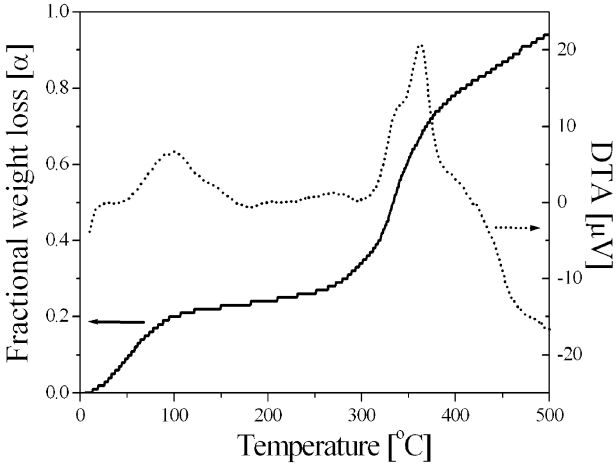

Fig. 6. The debinding profiles of 5 wt.% monomer concentrated green body (1.75 wt.% PAA, 50 vol.% solid loading) as a result of TG-DTA.

systems has already been investigated through a systematic study of the specific processes.[17,18] Complete reduction of NiO to Ni metal in the Al_2O_3/NiO green body was achieved by reduction at 700 °C with hydrogen gas (dew point −75 °C). The morphological characteristics of the Al_2O_3/5vol.%Ni reduced specimen observed by TEM are shown in Fig. 7. Fine spherical nickel particles of 20–30 nm appear as precipitates within the Al_2O_3 matrix, mainly at the surface of Al_2O_3. No shrinkage behavior was observed under these reduction conditions.

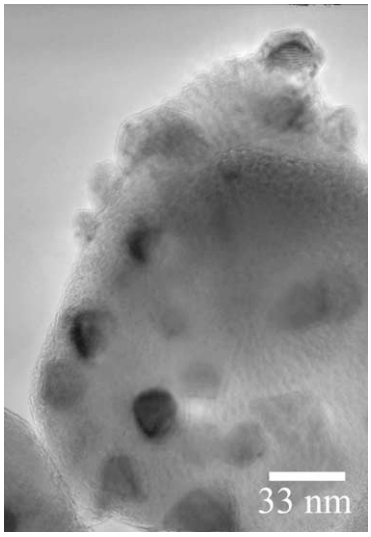

Fig. 7. The TEM morphology of hydrogen reduced Al_2O_3/5vol.%Ni nanocomposite.

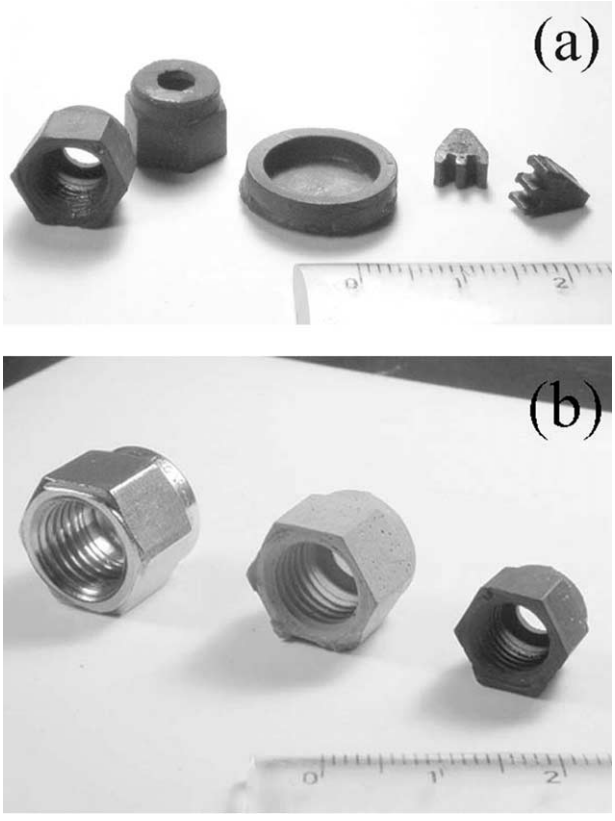

Fig. 8. Gelcasted final Al_2O_3/5 vol.%Ni nanocomposites; (a) various models of complex shaped specimens (nuts, cylinder, partitions of gear), and (b) volume changes at the related suspension casting, humid drying and reduction-sintering process.

Al_2O_3/5vol.%Ni nanocomposites of various shapes were successfully fabricated by pressureless sintering. Fig. 8 shows the various complex shapes fabricated by this process (a), and the change in volume of the nut-shaped specimen from molding, to drying and finally sintering (b). The total shrinkage of the nut-shaped specimen was 21.45%. The final density of the specimens was 99.27% of the theoretical value, and the three-point bending strength of the rectangular specimen was 586.94±50 MPa. Although the differences in methods and conditions for mechanical testing make it difficult to set up an appropriate comparison, the present pressureless sintering result is very close to results reported for pressure-assisted sintering of pure Al_2O_3 (605 MPa).[14]

Fig. 9 shows the fracture surface of the sintered Al_2O_3/5vol.%Ni nanocomposite, which has a relatively fine Al_2O_3 matrix and fine nickel particles. These microstructural and mechanical properties strongly suggest that dispersion of nano-sized Ni can contribute to the strengthening of Al_2O_3 through inhibition of grain growth[20] and grain boundary strengthening (Al_2O_3–Al_2O_3 and/or Al_2O_3–Ni).[21] The advantage of the gelcasting process is that it allows for homogeneous density distribution and matrix grain size in complex-shaped specimens.[10–12]

Fig. 10 shows a magnetic hysteresis loop for sintered Al_2O_3/5vol.%Ni nanocomposites. Dispersed Ni in gelcast Al_2O_3/5vol.%Ni nanocomposites produced ferromagnetism in the final specimen, with a saturation magnetization of 50.9 emu/g. The coercive force, 3.3 kA/m, is approximately two orders of magnitude larger than that of pure Ni (70 A/m), and is only slightly lower

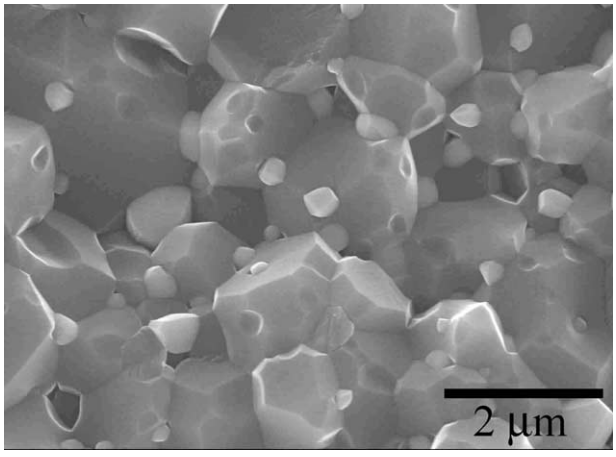

Fig. 9. The fracture surface of gelcasted Al_2O_3/5 vol.%/Ni nanocomposites.

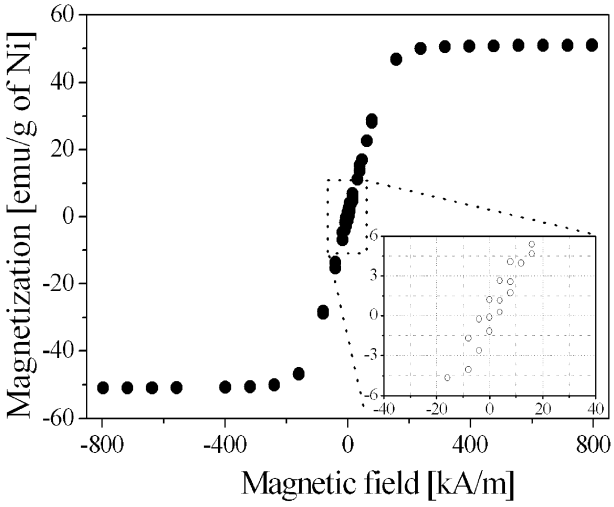

Fig. 10. Magnetic hysteresis loop of gelcasted Al_2O_3/5 vol.%/Ni nanocomposites.

than that of hot-pressed specimens[4] (4.4 kA/m, 1450 °C, 1 h) and pulse-current sintered specimens[22] (4.0 kA/m, 1450 °C, 5 min). Fine ferromagnetic Ni particles are known to exhibit high magnetic coercive force as a result of the characteristic magnetic domain structure.[23,24] As the particle size of a magnetic material decreases, the magnetic structure changes from multi-domain to single-domain through reduction of the total energy of the system. Although the Ni particle size in the present Al_2O_3/5vol.%Ni nanocomposite system is considered to be larger than that in pressure-assisted sintered specimens,[4,22] the coercive force enhancement in the present case is expected to be due to this size effect.

4. Conclusions

Gelcast Al_2O_3/Ni nanocomposites without degraded mechanical or functional magnetic properties were successfully fabricated. The gelcasting process conditions were optimized based on investigation of the basic processes involved, including the suspension parameters, drying behavior, debinding conditions, and reduction-sintering process. It was confirmed that the concentrations of monomer, dispersant, and solid strongly influence the rheological behavior of the Al_2O_3/NiO suspension. The optimal suspension conditions for the preparation of binary oxide green bodies of various shapes were found as follows: 1.75 wt.% dispersant, 50 vol.% solid, and 8 wt.% monomer. The wet body shrank by 4.72% upon drying in a humidity-controlled chamber, and the bending strength of the final dried body was about 3.84 MPa. Good Al_2O_3/Ni nanocomposites of various shapes and with ferromagnetic properties were successfully synthesized by hydrogen reduction of the debound body and continuous pressureless sintering. The density of the final specimens was 99.27% of the theoretical density, with 21.45% shrinkage and bending strength of 586 MPa after sintering. These results demonstrate that gelcasting is a viable technique for the synthesis of Al_2O_3/Ni nanocomposites in various complex shapes with high strength and magnetic functionality.

Acknowledgements

This work is partly supported by the Japan Society for the Promotion of Science (JSPS) under a Grant-in-Aid for Scientific Research, No13305049. The authors acknowledge Prof. Jai-Sung Lee of Hanyang University, Korea for his help for preparation of casting molds.

References

1. Niihara, K., New design concept of structural ceramics nanocomposites. *J. Ceram. Soc. Jpn.*, 1991, **99**, 974–982.
2. Nawa, M., Yamazaki, K., Sekino, T. and Niihara, K., Microstructure and mechanical behavior of 3Y-TZP/Mo nanocomposites processing a novel interpenetrated intragranular microstructure. *J. Mater. Sci.*, 1996, **31**, 2849–2858.
3. Choa, Y.-H., Nakayama, T., Sekino, T. and Niihara, K., Fabrication of nano-sized metal dispersed magnesia based composites and related mechanical and magnetic properties. *J. Kor. Ceram. Soc.*, 1999, **5**, 395–399.
4. Sekino, T. and Niihara, K., Microstructural characteristics and mechanical properties for Al_2O_3/metal nanocomposites. *NanoStr. Mater.*, 1995, **6**, 663–666.
5. Nawa, M., Sekino, T. and Niihara, K., Fabrication and mechanical behavior of Al_2O_3/Mo nanocomposite. *J. Mater. Sci.*, 1994, **29**, 3185–3192.
6. Hwang, H.-J., Toriyama, M., Sekino, T. and Niihara, K., In-situ fabrication of ceramic/metal nanocomposites by reduction reaction in barium titanate–metal oxide systems. *J. Eur. Ceram. Soc.*, 1998, **18**, 2193–2199.
7. Chen, R. Z. and Tuan, W. H., Pressureless sintering of Al_2O_3/Ni nanocomposite. *J. Eur. Ceram. Soc.*, 1999, **19**, 463–468.
8. Leverkoehne, M., Murthy, V. S. R., Janssen, R. and Claussen, N., Electrical resistivity of Cr–Al_2O_3 and Zr_xAl_y–Al_2O_3 composites with interpenetrating microstructure. *J. Eur. Ceram. Soc.*, 2002, **22**, 2149–2153.
9. Gao, L., Wang, H. Z., Hong, J. S., Miyamoto, H., Miyamoto, K., Nishikawa, Y. and Torre, S. D. D. L., Mechanical properties and microstructure of nano-SiC–Al_2O_3 composites densified by spark plasma sintering. *J. Eur. Ceram. Soc.*, 1999, **19**, 609–613.
10. Young, A. C., Omatete, O. O., Janney, M. A. and Menchhofer, P. A., Gelcasting of alumina. *J. Am. Ceram. Soc.*, 1991, **74**, 612–618.
11. Lewis, J. A., Colloidal processing of ceramics. *J. Am. Ceram. Soc.*, 2000, **83**, 2341–2359.
12. Gilissen, R., Erauw, J. P., Smolders, A., Vanswijgenhoven, E. and Luyten, J., Gelcasting, a near net shape technique. *Mater. & Design*, 2000, **21**, 251–257.
13. Laucournet, R., Pagnoux, C., Chartier, T. and Baumard, J. F., Coagulation method of aqueous concentrated alumina suspensions by thermal decomposition of hydroxyaluminum diacetate. *J. Am. Ceram. Soc.*, 2000, **83**, 2661–2667.
14. German, R. M., *Sintering Theory and Practice*. John Wiley and Sons, Oxford, 1996.

15. Ghosal, S., Emami-Naeini, A., Harn, Y. P., Draskovich, B. S. and Pollinger, J. P., A physical model for the drying of gelcast ceramic. *J. Am. Ceram. Soc.*, 1999, **82**, 513–520.
16. Scherer, G. W., Theory of drying. *J. Am. Ceram. Soc.*, 1990, **73**, 3–14.
17. Lee, J.-S. and Kim, B.-S., Synthesis and related kinetics of nanocrystalline Ni by hydrogen reduction of NiO. *Mater. Trans.*, 2000, **42**, 1607–1612.
18. Kim, B.-S., Lee, J.-S., Sekino, T., Choa, Y.-H. and Niihara, K., Hydrogen reduction behavior of NiO dispersoid during processing of Al_2O_3/Ni nanocomposites. *Scripta Materialia*, 2001, **44**, 2121–2125.
19. Brunauer, S., Emmett, P. and Teller, E., Adsorption of gases in multimolecular layers. *J. Am. Chem. Soc.*, 1938, **60**, 309–319.
20. Boras, C. E., Jiao, S., Todd, R. I. and Brook, R. J., Processing and properties of Al_2O_3/SiC nanocomposites. *J. Microscopy*, 1994, **177**, 1139–1148.
21. Jiao, S., Jenkins, M. L. and Davidge, R. W., Interfacial fracture energy-mechanical behavior relationship in Al_2O_3/SiC and Al_2O_3/TiN nanocomposite. *Acta Mater.*, 1997, **45**, 149–156.
22. Kim, B.-S., Sekino, T., Nakayama, T., Wada, M., Lee, J.-S. and Niihara, K., Pulse electric current sintering of alumina/nickel nanocomposites. *Mater. Res. Innov.*, 2003, **7**, 57–62.
23. Yermakov, A. Y. E., Ivanov, O. A., Shur, Y. A. S., Grechishkin, R. M. and Ivanova, G. V., Magnetic properties of nanocrystalline powders of nickel. *Phys. Met. Metall.*, 1972, **33**, 99–104.
24. Kamel, R. and Reffat, A., On the effect of lattice disorders on the reversible magnetization process in pure nickel. *Solid State Commu*, 1970, **8**, 821–823.